Collision-induced dissociation and dissociative capture of H_2^+ in Ar and Kr

H. Martínez[1] and F. B. Yousif[2,*]

[1]*Centro de Ciencias Físicas, Universidad Nacional Autónoma de México, Cuernavaca, Morelos, P.O. Box 48-3, 62251, Cuernavaca, Morelos, Mexico*

[2]*Facultad de Ciencias, Universidad Autónoma del Estado de Morelos, Avenida Universidad 1001, 62210, Cuernavaca, Morelos, Mexico*

(Received 15 November 2003; revised manuscript received 26 January 2004; published 2 June 2004)

Measurements of the absolute total and differential cross sections for the production of protons and hydrogen atoms in the energy range of 1–5 keV for reactions of H_2^+ molecular ions in Ar and Kr targets are reported. The results show that the cross section for the dissociative capture (DC) proccess is about one order of magnitude higher than that for the collision-induced dissociation. The angular distribution of the fragments in both targets and for all acceleration energies shows a monotonic decrease in the differential cross section with increasing angle. A sharp increase in the angular distribution at scattering angles $<1.6°$ is observed for hydrogen atoms resulting from DC and in particular for the Kr target.

DOI: 10.1103/PhysRevA.69.062701 PACS number(s): 34.50.−s, 34.70.+e

I. INTRODUCTION

Collision of fast molecular ions with target atoms is a subject of fundamental interest as well as of importance for fields such as astronomy, chemical reactions, and most importantly plasma injection heating. In collisions of molecular ions with target atoms, several competing reactions are involved such as dissociation, ionization, and electron capture. The importance of each of these reactions is dependent upon the initial state of the molecular ions as well as on the collisional energy.

Several experiments have been reported on the collisional dissociation of H_2^+ ions [1–6] in the keV–MeV energy range and mainly proton production cross sections were measured. Among those, considerable differences are found to exist in the measured cross sections. Bates and Holt [7] and Peek [8] employed the Born approximation to qualitatively explain the energy and angular distribution of the dissociated fragments. However, satisfactory explanations for the competing processes were not obtained especially in the in the lower-keV region. In the lower-keV energies, collisions of H_2^+ with several target atoms were investigated experimentally [9] between 4 and 16 keV, and data for charged and neutral fragments below 10 keV are clearly scarce. More importantly, there is a serious need for angular distributions of the neutral fragments which can be carried out in this laboratory. Measurements were obtained for collisional-induced dissociation (CID) and dissociative capture (DC) for H_2^+ ions in collisions with Ar and Kr targets bellow 5 keV. The angular distributions for both protons and neutral fragments are reported within ±7°.

II. EXPERIMENTAL APPARATUS

The experimental apparatus employed in the present investigation has been described in detail elsewhere [10] and a brief description is made here. As shown in Fig. 1, it consists of three sections: the ion source, the scattering chamber, and the rotating section which house the analysis and detection region. The H_2^+ molecular ions are generated in a Colutron-type ion source with the injection of a research-grade mixture of hydrogen and Ar gases. The Ar gas, which constitutes 25% of the mixture, is needed to enable the cathode-anode discharge.

The H_2^+ ions were focused and accelerated to the desired energy. A typical H_2^+ beam intensity of about 10^{-8} A at 5 keV was obtained. Beam collimation reduced the beam intensity to about 10^{-10} A. The focused beam was passed into a Wien velocity filter in order to have analyzed ions with the desired velocity. Following that, the ions were deflected 10° with respect to the initial trajectory using two sets of electrostatic plates in order to avoid the detection of the photons generated the ion source filament by the particle detector. The 2.54-cm-long and 2.54-cm-diam cylindrical target cell is contained within the scattering chamber. The exit aperture of the target cell is 2 mm in diameter and 6 mm long. This allows the detection of the dissociated fragments within ±7° with respect to the trajectory of the incoming beam.

The detection system consisted of a parallel-plate analyzer and two-channel electron multipliers (CEM's). The system is located 47 cm away from the target cell. The entire system is rotatable using a computer-controlled stepper motor. The target cell is at the center of curvature of the rotation. The precision stepper motor ensured high-precision reproducibility in the positioning of the chamber. Path length and apertures were chosen such that the root mean square of the angular resolution of the system was evaluated to be 0.1°. The parallel-plate analyzer entrance aperature is 0.36 mm in diameter and the two CEM's are attached to its exit ends. The trajectory of the ion beam makes an angle of 45° with respect to the front plate of the analyzer, while the resulting neutrals pass through the analyzer 1-cm-diam exit orifice at the rear end plate and strike the CEM. This flux served throughout the experimental work as a measure of the stability of the ion beam. The separation of the charged particles occurred inside the analyzer and they were detected by the lateral CEM. The multiplier counting efficiency data for H^+, previously measured [11], were used to correct for our measured signals. The detection efficiency for H^0 was assumed to be the same as that of H^+ at the same energy. The intensity

*Electronic address: fbyousif@servm.fc.uaem.mx

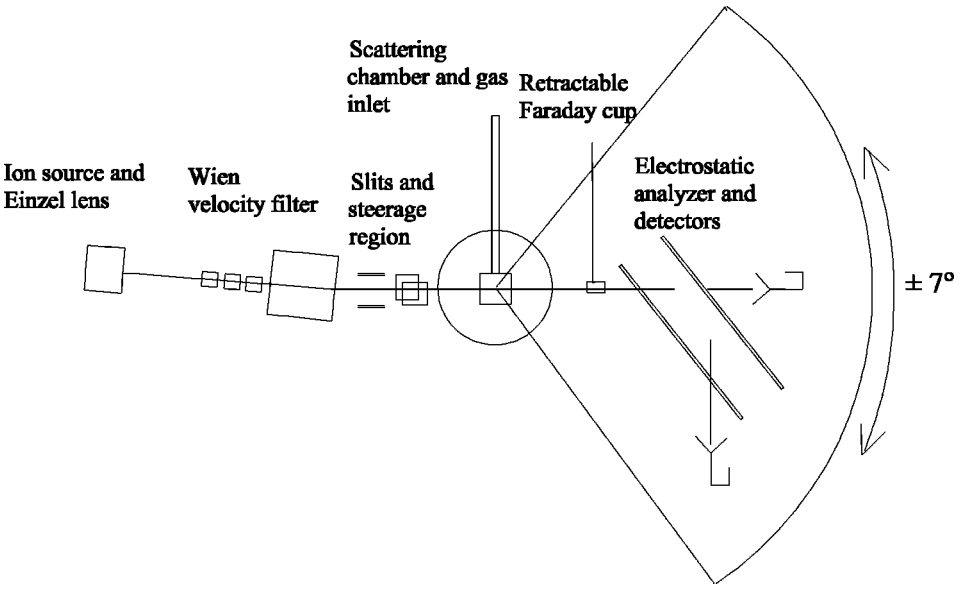

FIG. 1. Schematic diagram of the experimental apparatus.

of the H_2^+ ion beam was measured by the use of a retractable Faraday cup located 32 cm down stream from the target cell. Typical ion currents of 10^{-10} A were measured using a Kiethley Instrument Electrometer model 610C. During the course of experimental measurements, a vacuum base pressure of 2×10^{-7} Torr was maintained without gas in and 1×10^{-6} Torr with gas in the cell.

III. RESULTS AND DISCUSSION

Hydrogen is the most abundant element in the Universe and much of it exists in molecular form. When molecular hydrogen is ionized, H_2^+ is formed, and in collisions with target atoms, the H_2^+ undergoes the following processes:

$$H_2^+ + X \rightarrow H^0 + H^0 + X^+, \quad (1)$$

$$H_2^+ + X \rightarrow H^+ + H^0 + X, \quad (2)$$

and

$$H_2^+ + X \rightarrow H^+ + H^+ + X + e. \quad (3)$$

All of the above processes contribute the measured signals of protons and neutral atoms. They are identified as DC, CID, and electron loss followed by Coulomb explosion (CE), respectively. Our measured total cross sections for the H^+ and H^0 production in collisions with Ar and Kr targets are plotted in Figs. 2–4 as a function of acceleration energy. Shown also are the results of other groups for comparison. Also included in Fig. 2, the data corresponding to CID and CE from Guidini [4] corresponding to reactions (2) and (3), respectively, as well as those of from Suzuki *et al.* [12] for reaction (3).

Suzuki *et al.* [12] measured the ratio of reactions (2) and (3) and found it to be 4.4 at 4 keV with 50% error bars associated with reaction (3), indicating low signal levels. A high ratio such as this is expected since H_2^+ requires about 35 eV in excitation energy to lose the remaining electron and for Coulomb explosion to follow [reaction (3)]. This process is expected to be considerably weaker than the excitation of the $H_2^+[^2\Sigma_g^+\ (\nu=0)]$ to the repulsive $2P\sigma_u$, which requires only about 12 eV. Therefore the possible contribution of reaction (3) to our total measured CID signal is expected to be about 20% at the high-energy limit and is expected to be less than that at the lower acceleration energies. Our present CID data are not corrected to take into account the effect of reaction (3).

Figures 2 and 3 for H^+ and H^0 production in Ar targets show the serious discrepancies among the previously mea-

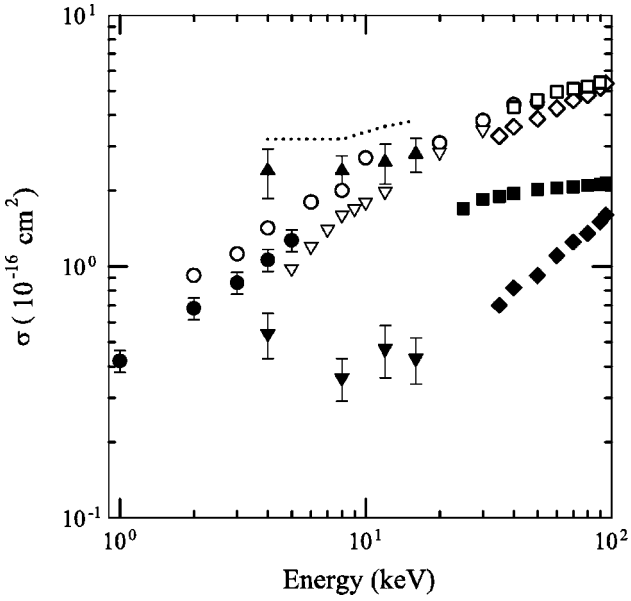

FIG. 2. Total cross section for the production of H^+ fragments in H_2^+-Ar collisions. Solid squares: total CID [4]. Solid diamonds: protons resulting from reaction (3) [4]. Solid up triangles: total CID [12]. Solid down triangles: protons resulting from reaction (3) [12]. Sold circles: present results for H^+ total cross section. Open diamonds: H^+ formation [4]. Dotted line: H^+ formation [12]. Open circles: H^+ formation [15]. Open down triangles: H^+ formation [2]. Open squares: H^+ [3].

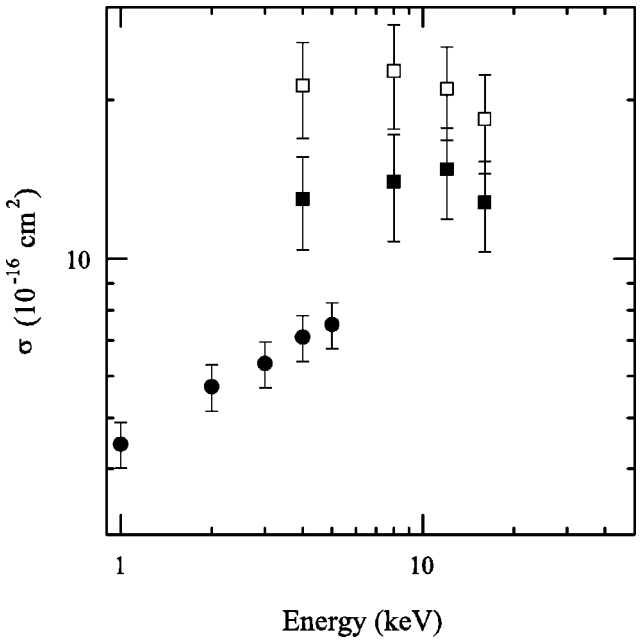

FIG. 3. Total cross section for the production of H^0 fragments in H_2^+-Ar collisions. Solid squares: H^0 [12]. Open squares: (CID +DC) [12]. Solid circles: present results for total H^0.

sured cross sections. These discrepancies are likely due to the fact that molecular ions are usually formed within ion sources in a variety of vibrationally excited states. The population of these states at any given time will depend upon the collisional history of the ions. However, since the H_2^+ ions do not have a dipole moment, therefore these vibrationally excited states have very long lifetimes ($\simeq 10^6$ s) and so do not decay; yet it is possible to alter and even remove the

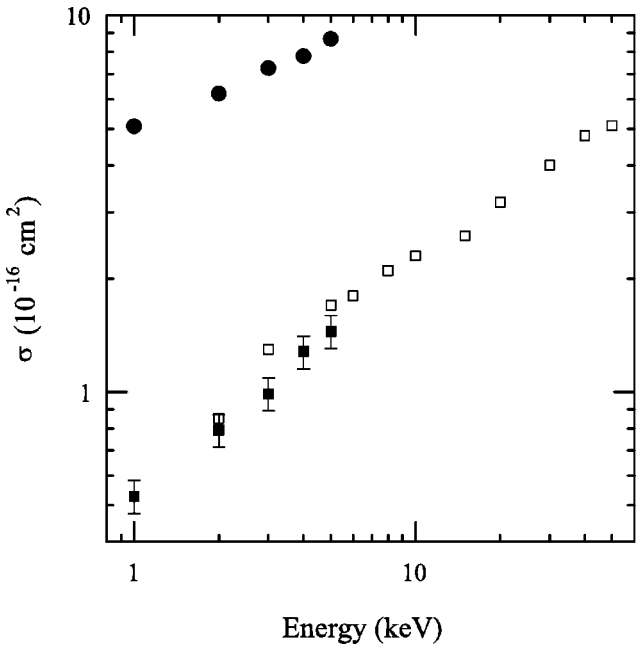

FIG. 4. H_2^+-Kr collisions. Solid squares: present results for total H^+. Open squares: total H^+ [15]. Solid circles: present result for total H^0 fragments.

excited vibrational states reactively by allowing the H_2^+ ions to react with rare gases within the ion source [13].

Eventually, since the ion source used in this work is that of electron bombardment, it is expected that all 18th vibrational levels will be populated [14] although the relative population of these vibrational levels cannot be determined within the present experimental apparatus.

For the H^+ fragments cross section in an Ar target shown in Fig. 2, our measurements extending up to 5 keV appear to merge well with those at the lower-energy-limit measurements of Fedorenko *et al.* [1] and about 20% lower than those of Williams and Dunbar [15], while there is a serious disagreement between our measured cross sections and those of Suzuki *et al.* [12].

Discrepancies are apparent for the H^0 fragments in an Ar target as seen in Fig. 3. The results of Suzuki *et al.* [12] at 4 and 5 keV collisional energies are a factor of 2 higher than our measured cross sections at the same energies. For the Kr target, our results for H^+ shown in Fig. 4 extend well enough with those of Williams [15], while our total fragment cross sections are found to show a monotonic increasing behavior as a function of acceleration energy (see Fig. 4) and we are aware of no previous experimental or theoretical data regarding H^0 formation to compare with the present results.

The excitation route for the CID is dependent on the excitation energy, yet all possible excitations to states below the second ionization energy would result in a hydrogen atom and proton [3]. Therefore the excitation mechanisms involved in the CID are either the electronic excitation to a repulsive state—mainly to the $2P\sigma_u$—or the vibrational excitation. Traditionally measurements of the kinetic energy release are often used to identify the final repulsive excited states.

Given the fact that the CID results in an equal number of protons and hydrogen atoms, therefore the absolute DC cross section can be obtained by subtracting the number of measured protons from the total neutrals assuming low collisional energies in which other processes such as the H_2^{++} production are week compared to DC and CID [12]. Our measured cross sections for CID and DC leading to H^+ and H^0 in Ar and Kr targets are shown in Fig. 5. Both cross sections for Ar and Kr targets show the same behavior with those for the Kr target slightly higher than those for the Ar target, while for both targets, the DC process is approximately one order of magnitude higher than that for CID and eventually 20 times that of reaction (3).

Measurements on charge exchange and dissociation cross sections for H_2^+ in inert gases [15] showed similar trend regarding the ratio of H^0 to H^+ at energies between 6 and 50 keV; the H^0 production was shown to be about 4 times higher than that for the H^+.

The second part of this work involved the angular distribution of the dissociating fragments. The differential cross sections for the fragments formation under single-collision conditions were evaluated from the measured quantities by using the expression

$$\frac{d\sigma(\theta)}{d\Omega} = \frac{I_f(\theta)}{I_0 nl}, \tag{4}$$

where I_0 is the number of H_2^+ ions traversing the target, n is the number of Ar or Kr target atoms per unit volume, l is the

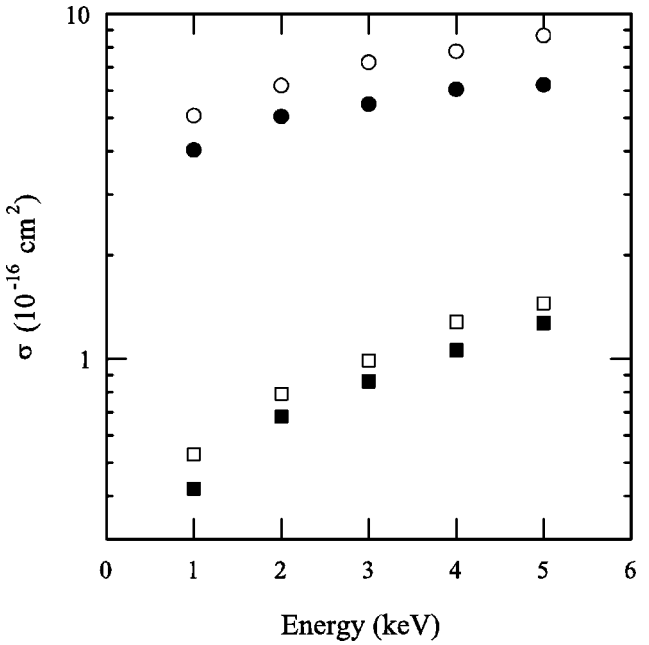

FIG. 5. H_2^+ in Ar and Kr collisions. Solid circles and squares are for DC and CID in an Ar target, respectively, and open circles and squares are for DC and CID in a Kr target, respectively.

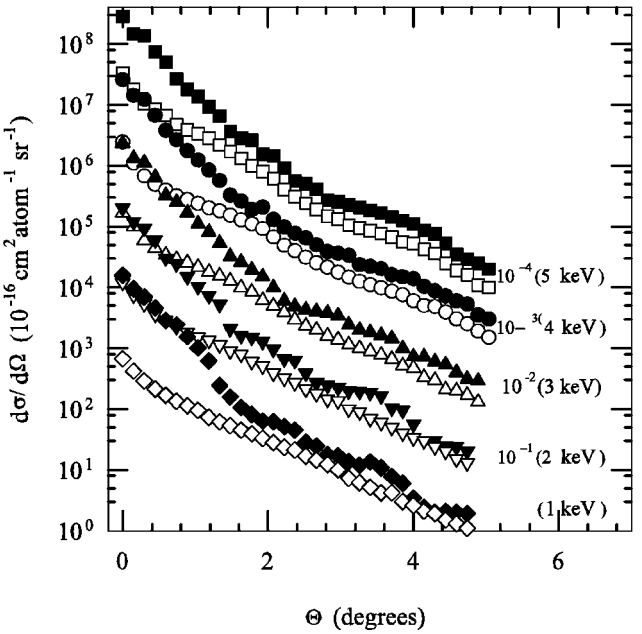

FIG. 6. Angular distribution for H^0 and H^+ corresponding to DC (solid symbols) and CID (open symbols) in an Ar target for acceleration energies 1–5 keV.

length of the scattering chamber (2.54 cm), and $I_f(\theta)$ is the number of H^+ or H^0 fragments per unit solid angle per second detected at the laboratory angle θ with respect to the incident beam direction. The total cross section σ for the production of H^+ or H^0 fragments is evaluated by the integration of $d\sigma/d\Omega$ over all the range of angles as

$$\sigma = 2\pi \int_0^{\pi} \frac{d\sigma(\theta)}{d\Omega} \sin(\theta) d\theta. \tag{5}$$

The count rate due to the background distribution was eliminated by subtracting the angular distribution measurements made with the gas off from those made with gas on. The H_2^+ ion beam intensity was measured before and after each angular scan. The symmetry of the angular distributions was verified by conducting measurements on both sides of the forward direction. The overall error is estimated to be 15%, while the total cross sections reproducibility was found to be within 10%. The contribution of the neglect of reaction (3) to the measured cross sections is estimated to be about 20% to CID and 2% to DC cross sections.

Considering the fact that the $d\sigma(\theta)/d\Omega$ looks like a differential cross section and is measured as such, yet it is not a "differential scattering" cross section. The angle the fragments acquired at the detector is due to the transverse component of the velocity that acquired in the dissociation process.

The differential cross sections for H^+ fragments (CID) and H^0 fragments (DC) in Ar and Kr targets were obtained as outlined earlier at low collisional energies and are shown in Figs. 6 and 7.

It can be seen that all the data show a monotonic decrease in the differential cross sections with increasing angle. In both targets, for H^+ formation, the increase in acceleration energy from 1 to 5 keV results in an increase of one order of magnitude in the differential cross section, while for H^0 formation, the increase in the differential cross sections is of a factor of 2. For all acceleration energies and at all scattering angles, the DC/CID ratio is larger than unity. A ratio of about 2 is observed to remain constant for scattering angles above 1.6°. At angles $<1.6°$, the ratio increases significantly. Also below a 1.6° scattering angle, there is a gradual increase of the ratio as a function of descending acceleration energies for both targets. Figure 8 shows such behavior for the Kr target

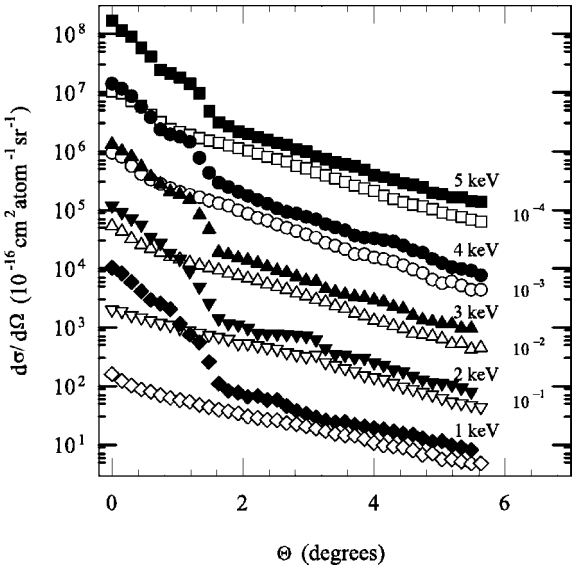

FIG. 7. Angular distribution for H^0 and H^+ corresponding to DC (solid symbols) and CID (open symbols) in a Kr target for acceleration energies 1–5 keV.

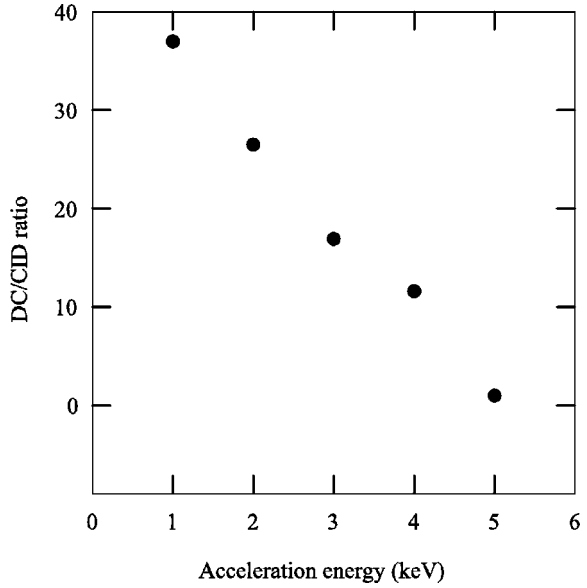

FIG. 8. DC/CID ratio at 0.6° as a function of acceleration energy in a Kr target.

at 0.6° scattering angle. It can be seen that the ratio at 1 keV acceleration energy is more than one order of magnitude larger than that at 5 keV.

Recently, Itzik Ben-Itzhak [16] indeed showed that the two processes of DC and CID are dependent on the initial state of the H_2^+ ions. In his work, the two processes were separated experimentally employing three-dimensional momentum imaging of the fragments. Furthermore, CID caused by an electronic excitation to a repulsive state is distinguished from that caused by vibrational excitation, by the difference in momentum transfer to the projectile. Also it was shown that the electronic CID is orders of magnitude higher than that of vibrational CID. Therefore, within the low collisional energies of the present work, it is possible to assume that DC and the electronic CID are the only processes involved. He also showed that in the case of H_2^+, both, electronic and vibrational CID are strongly favored for molecular ions aligned perpendicular to the beam direction and their dissociation is along the momentum transfer with vibrational CID to contribute very little to the measured signal. This would correspond to our measured signal at scattering angle larger than 1.6°. In contrast, it was found [16] that the DC strongly favors molecules aligned along their velocity ($\Theta = 0°$) and dominating their measured signal and dissociate along the velocity vector. With a very large kinetic energy release up to 8 eV [16], this would correspond to our measured angular distribution at $\Theta < 1.6°$ and confirm our higher ratio of DC/CID below 1.6°.

IV. CONCLUSION

We report the collisional reactions of H_2^+ molecular ions in Ar and Kr with measurements of the absolute total cross section resulting in protons and hydrogen atoms in the energy range of 1–5 keV as well as angular distributions of the resulting fragments.

The two main processes involved are the DC and the electronic CID. The measured total absolute cross sections show that the dissociative capture proccess within the acceleration energy range of this work to be higher than that of collision-induced dissociation. Our measured cross sections in Kr targets are reported for the first time. The DC/CID ratio was found to remain practically constant for scattering angles $>1.6°$ and for all acceleration energies. A sharp increase in the DC/CID ratio is observed at scattering angles $<1.6°$. This increase in the cross section ratio was found to be more pronounced in the case of Kr targets.

ACKNOWLEDGMENTS

The authors are grateful to A. Bustos, A. Gonzalez, and Jose Rangel for technical assistance. We are grateful to F. Castillo for helpful suggestions and comments. This research was supported by DGAPA IN-109103-3 and CONACyT 41072-F as well as PROMEP and PIFI2

[1] N. V. Fedorenko, V. V. Afrosimov, R. I. IL'in, and D. M. Kaminker, Zh. Eksp. Teor. Fiz. **36**, 385 (1959); Sov. Phys. JETP **9**, 267 (1959).
[2] N. V. Fedorenko, J. Tech. Phys. **24**, 769 (1954).
[3] D. R. Sweetman, Proc. R. Soc. London, Ser. A **256**, 416 (1960).
[4] J. Guidini, Compt. Rend. **253**, 829 (1961).
[5] R. I. IL'in, B. I. Kikiani, V. A. Oparin, E. S. Solov'ev, and N. V. Federnko, Zh. Eksp. Teor. Fiz. **46**, 1208 (1964) [Sov. Phys. JETP **19**, 817 (1964)].
[6] H. S. W. Massey, E. H. S. Burhop, and H. G. Gilbody, *Electronic and Ionic Impact Phenomena*, 2nd ed. (Oxford University Press, London, 1974), Vol. 5.
[7] D. R. Bates and A. R. Holt, Proc. Phys. Soc. London **85**, 691 (1965).
[8] J. M. Peek, Phys. Rev. **140**, A11 (1965).
[9] S. Yasufumi, K. Takeomi, T. Michio, and S. Masakatsu, J. Phys. Soc. Jpn. **55**, 3037 (1986).
[10] H. Martinez and P. G. Reyes, Int. J. Mass Spectrom. Ion Processes **173**, 17 (1998).
[11] D. H. Crandall, J. A. Ray, and C. Cisneros, Rev. Sci. Instrum. **46**, 562 (1975).
[12] Y. Suzuki, T. Kaneko, and M. Sakisaka, Nucl. Instrum. Methods Phys. Res. B **16**, 397 (1986).
[13] H. Hus, F. B. Yousif, C. Noren, and J. B. A. Mitchell, Phys. Rev. Lett. **60**, 1006 (1988).
[14] F. Von Busch and G. H. Dunn, Phys. Rev. A **5**, 1726 (1972).
[15] J. F. Williams and D. N. F. Dunbar, Phys. Rev. **149**, 62 (1966).
[16] Itzik Ben-Itzhak (unpublished).